

3D Printed Pyramidal Horn Antennas

Majid Ahmed

Student

American University of Sharjah

Sharjah, UAE

b00077868@aus.edu

Abstract—This paper describes the process of designing and fabricating low-cost 3D-printed pyramidal horn antennas. Typical horn antennas are created from a conductive metal that is machined to the desired shape. Nevertheless, pyramidal horn antennas designed to operate at 3 GHz with a gain greater than 15 dB were 3D printed and evaluated for their performance. The designed antennas were first simulated using Ansys Electronics, and then 3D printed using a Fused Deposition Modeling (FDM) 3D printer. A layer of resin was then applied to the prototypes' inner surfaces, followed by conductive tape to finalize the design for measurements. The measurements indicate that 3D printing can be crucial in making inexpensive microwave equipment available for educational and hobbyist purposes.

Index Terms—Pyramidal horn antenna, 3D printed antenna, Additive manufacturing, Microwave circuits, Antennas

I. INTRODUCTION

Horn antennas are directional antennas used for numerous applications requiring moderate gain and high bandwidth, such as antenna parameter measurements and as feeds for reflector antennas which are used a lot for satellite communications. A typical horn antenna comprises a waveguide followed by a flared antenna, which can be a conical, rectangular, or corrugated horn. For instance, a typical pyramidal horn antenna is flared on all sides, making its cross-section rectangular. The antenna is flared such that the impedance mismatch that electromagnetic waves experience is decreased when transitioning from the antenna to the transmission/reception medium.

The impedance matching effect in horn antennas is achieved by making the electromagnetic waves experience a gradual change in the wave impedance of the propagation medium such that it nears the impedance of free propagation. Consequently, a horn antenna can be considered an impedance-matching device that matches the impedance of the waveguide to that of free space while also directing the electromagnetic waves into a narrower beam.

A typical horn antenna is made of a conductive metal machined to the desired antenna dimensions. The costs of the materials required and machining are relatively high to meet the necessary tolerances, as any irregularities in the antenna surface can result in undesired phase changes inside the antenna, which would alter its radiation properties. This paper aims to design and evaluate a pyramidal horn antenna that costs less than 30 USD to manufacture. The recent advances in 3D printing have made it possible to fabricate models with

varying complexities. Hence, 3D printing is a technique that can be used to fabricate antennas within any given budget.

II. ADDITIVE MANUFACTURING

3D printing is an additive manufacturing process that involves depositing the desired raw material to create a 3D model. Thus, most of the raw material is used in making the model, leaving virtually no waste other than that used for any required supporting structure. Further, numerous techniques of 3D printing utilize different technologies to suit the choice of raw materials such as plastics, resins, or metals. Fusion Deposition Modelling (FDM) is a 3D printing technique by which a plastic filament is heated up and layered on a build plate to produce the desired model. FDM is the most used 3D printing technique due to the variety of plastic filaments and 3D printers available on the market. Nevertheless, FDM is mainly used for quick prototyping due to its limited resolution, which is dictated by the deposited layers' height. FDM was the 3D printing technique of choice due to the low price of the plastic filament.

FDM 3D printers operate comparably regardless of brand. A plastic filament is heated up and extruded through a nozzle onto the printer's heated build plate. The most common types of plastic filaments used are acrylonitrile butadiene styrene (ABS), polylactic acid (PLA), and polyethylene terephthalate glycol (PETG). ABS is a non-flexible plastic used for applications requiring rigidity and a relatively high temperature tolerance. Further, PETG is a 3D printing filament derived from polyethylene terephthalate (PET), the same material used to make most water and soda bottles, with the addition of glycol to reduce cloudiness while improving the printed models' robustness. PETG has more tensile strength than ABS, as ABS suffers from poor interlayer adhesion. Lastly, PLA is the most used 3D printing filament due to its low price and ease of use. However, PLA is considerably more brittle than the other filaments, and its temperature resistance is lower.

Although FDM 3D printing can help create the desired antenna shape, most filaments are made of dielectric plastics. Thus, the models cannot be directly used as antennas. There are multiple conductive filaments available for FDM printers. However, they suffer from low conductivity, and using such filaments directly ties the performance of the printed antennas to the resolution of the 3D printer. Further, it is hard to ensure constant conductivity throughout the printed model.

On the other hand, covering the surface area of the dielectric models with a conductive layer is much more practical and cheaper, especially at moderately high frequencies due to the low skin depth, which causes most of the current density to be at the conductor's surface. For instance, the models can be electroplated with a copper layer, as discussed in [1, 2]. Further, conductive paint or conductive tape can be used to coat the model's surface. In addition, to overcome the low resolution of an FDM 3D printer, the model's surface can be sanded down, or a resin layer can be applied to smoothen the surface.

III. ANTENNA DESIGN AND SIMULATION

The size limitations of the pyramidal horn antenna were dictated by the maximum available build size of the utilized FDM 3D printer, which is 220mmx220mmx250mm. A center frequency of 3 GHz was chosen for the horn antenna design due to its large wavelength of 0.1 m, allowing printing of the antenna in a lower resolution of 0.2 mm. Consequently, the lower resolution-induced surface irregularities effects on the radiation properties are minimized. The surface roughness is expected not to introduce a significant phase transition even if left untreated by applying a resin layer or sanding. In addition, the designed antenna was attached to a WR-284 S-band waveguide with a length of 76.2mm. A Pasternack-manufactured waveguide in the 2.6-3.95 GHz frequency range was utilized. Lastly, the antenna was designed to have linear polarization. Two horn antennas were designed, and their performance was simulated using Ansys Electronics.

A. Ansys Electronics Simulations

The first horn antenna was designed with an additional 36.4mm added to the waveguide length. This was performed to examine the effects of such an addition on the real-world performance of the antenna. In addition, the antenna was designed to have a gain of 15.65 dB and a half-power beamwidth of 29.0 degrees at 3 GHz. This performance was achieved by creating a pyramidal horn antenna with a 200mmx175mm cross-section and a length of 188mm. The simulation indicates that the antenna has a broad bandwidth, but the utilized waveguide is expected to limit the actual bandwidth. Fig.1 (a) shows the simulated 2D radiation pattern, and Fig.1 (b) shows the simulated return loss plot of the first horn antenna. For the remainder of this paper, this antenna will be dubbed as the black horn antenna.

The second horn antenna was designed similarly but without the addition of an extra waveguide section. The designed antenna had a cross-section of 203mmx152mm and a length of 220mm. The simulation indicates a gain of 15.96 dB and a half power beamwidth of 31 degrees at 3 GHz. Fig.2 (a) shows the simulated 2D radiation pattern and Fig.2 (b) shows the simulated return loss plot of the second horn antenna. For the remainder of this paper, this antenna will be dubbed as the red horn antenna.

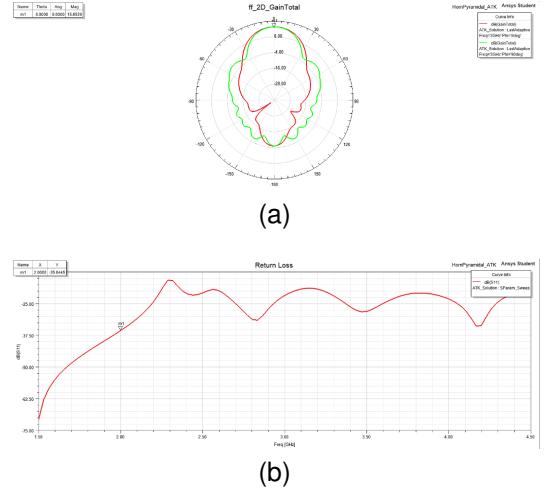


Fig. 1. First (Black) Horn Antenna Simulated (a) 2D Radiation Pattern (b) Return Loss.

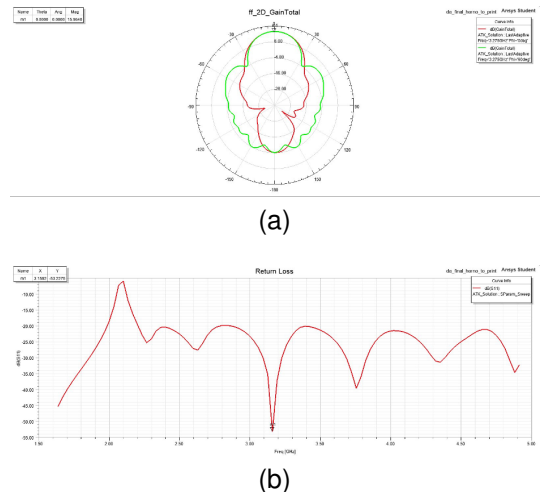
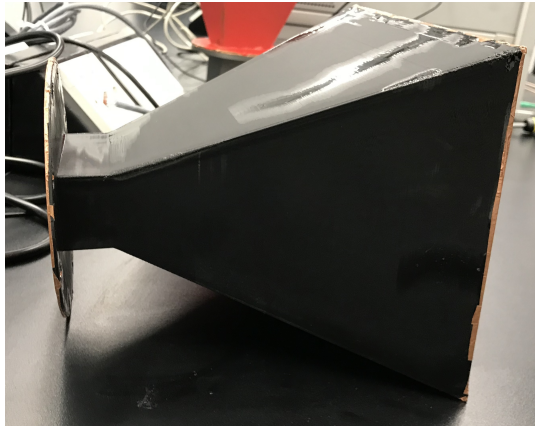


Fig. 2. Second (Red) Horn Antenna Simulated (a) 2D Radiation Pattern (b) Return Loss.

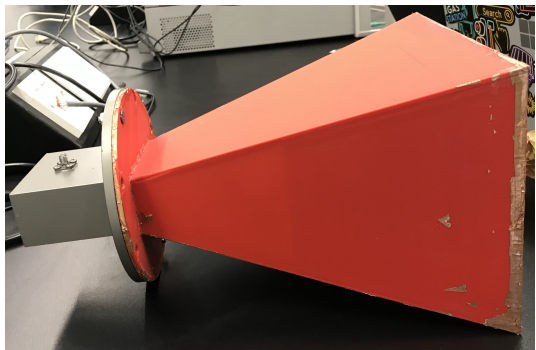
IV. ANTENNA FABRICATION AND EVALUATION

After the antenna designs had been finalized, 3D models of the antennas were created using Autodesk Fusion 360. The models were then exported to an appropriate 3D printing slicing software to divide each model into layers of the desired height. The layer height was set to 0.2 mm, and PLA filament was used to print the models. Each of the models took an average of 13 hours to print. Due to the relatively large layer height used, the final printed antennas were expected to have a high surface roughness due to the low printing resolution. This would result in unwanted phase changes inside the antenna, negatively affecting the radiation pattern. To solve this, the inner surface area of both antennas was coated using a simple resin mixture. However, sanding the antenna's inner surface or chemically smoothing it could be a viable solution. After coating, conductive copper tape was applied to the inner surface of the antenna. This turns the surface of the structure made up of a dielectric material conductive such that it can be

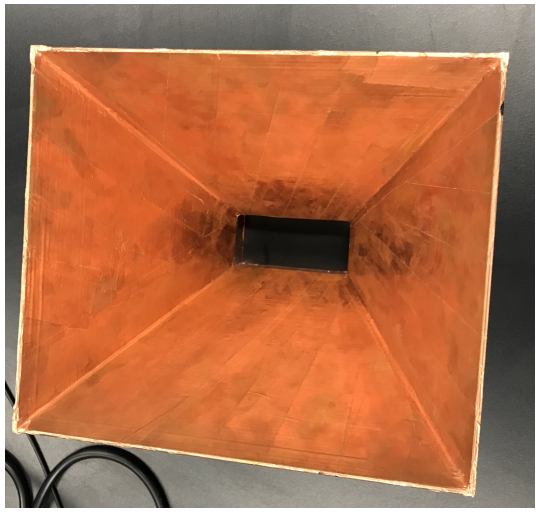
used as an antenna. Fig.3 (a) shows the first horn antenna in which the waveguide length is increased printed using black PLA filament, while Fig.3 (b) shows the second horn antenna printed using red PLA filament. It was observed that some irregularities have formed on the surface due to the presence of air bubbles in the resin after mixing.



(a)



(b)



(c)

Fig. 3. 3D Fabricated Antennas. (a) First (Black) Horn Antenna, (b) Second (Red) Horn antenna, and (c) top-view image.

A. Antenna Measurements

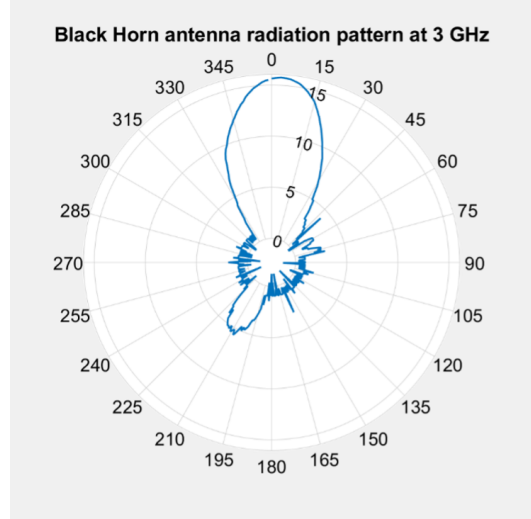
The methodology followed for measuring the gain of the designed antennas was the two-antenna method, as described in Constantine [3]. A reference ridged horn antenna with a gain of 11.5 dB at 3 GHz was used as the transmitting antenna. The transmitting antenna was fixed in its place at the same height as the receiving antenna. The designed models were placed on an antenna training system to enable rotation with 1-degree steps. A function generator was utilized as a radiofrequency source to output an amplitude-modulated 3 GHz wave with a power level of 7dBm and a modulating on-off frequency of 1 KHz. The separation distance between the transmitting and receiving antennas was set to 1.6m to ensure that both antennas were in the far field with respect to each other. Further, a vector network analyzer was used to measure the return loss of both antennas on a frequency range of 1-5 GHz. It must be noted that the measurements were not performed in an anechoic chamber, which would have omitted reflections from any reflective surface. Hence, the accuracy of the measurements is limited, but this should give an idea about the antenna characteristics. Fig.4 shows the experimental setup for the two-antenna method.



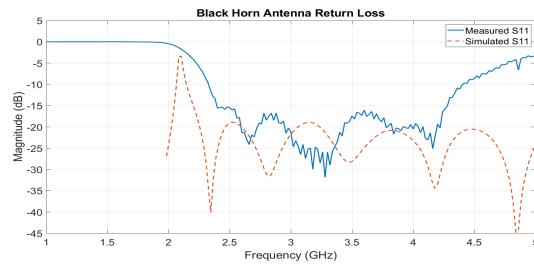
Fig. 4. 2-Antenna method Radiation Pattern Setup.

The measurements performed on the black horn antenna, which has an increased waveguide length, resulted in a maximum gain of 15.8 dB at 3 GHz, as shown in Fig.5 (a). The side lobe level, which is the difference in gain between the main lobe and the most prominent side lobe, was found as 10.1 dB. Further, the half-power beamwidth was calculated as 32.0 degrees. Lastly, the Return loss plot at Fig.5 (b) indicates that the designed horn antenna has a -10.0 dB bandwidth of 2.074 GHz centered at 3.36 GHz at which the reflection coefficient of the antenna is below -10 dB.

In addition, the measurements performed on the second horn antenna, which had larger dimensions without any addition to the waveguide length, resulted in a maximum gain of 16.5 dB at 3.0 GHz, as shown in Fig.6 (a). The gain is greater than the first horn antenna due to the increased antenna cross-section and length, which increased the gradual transitions of the electromagnetic radiation from the antenna to air. This



(a)



(b)

Fig. 5. Black Horn Antenna Measured (a) Radiation Pattern and (b) Return Loss.

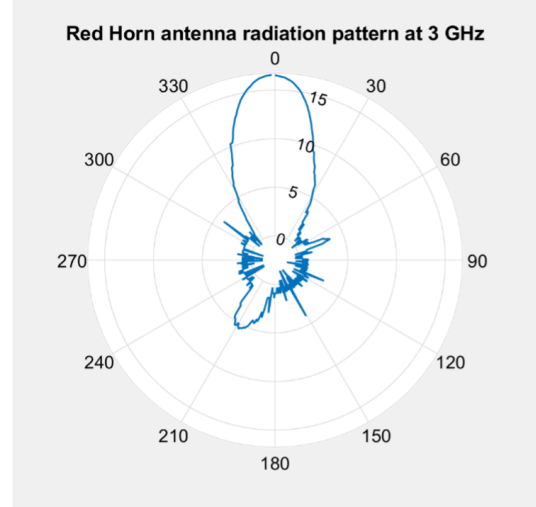
is further observed in Fig.6 (b), which depicts the return loss of the antenna. The return loss reaches a minimum reflection coefficient of -42.9 dB compared to the minimum reflection coefficient of the first antenna at -31.8 dB. Further, the measurements indicate a sidelobe level of 11.0 dB and a half-power beamwidth of 27.0 degrees.

V. CONCLUSION

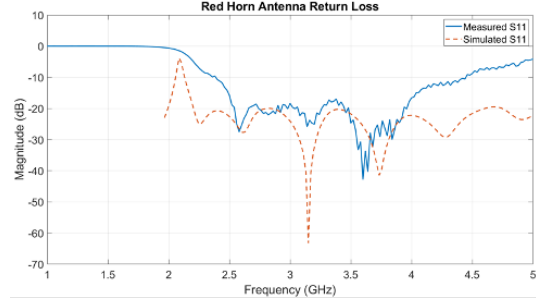
The measurement results indicate the feasibility of fabricating 3D-printed horn antennas. However, a rather unexpected sidelobe appeared on both horn antennas. This could be because the 3D-printed antennas are not perfectly attached to the utilized waveguide, which could have allowed some radiation to escape through a small opening. Further, the air bubbles in the applied resin mixture have resulted in minor irregularities on the inner surface of the antennas. This can be solved by putting the resin mixture in a vacuum chamber before applying it and by sanding the surface of the antenna.

In addition, printing the models in a higher resolution would help minimize the surface layer lines. Hence, if microwave circuits operating at sub-millimeter wavelengths are to be 3D printed, it is advisable to avoid using FDM 3D printing. Since most antennas at such high frequencies are physically small, stereolithography (SLA) 3D printing is a better

choice due to its higher resolution—furthermore, the antenna's higher resolution and small physical size ease electroplating. Lastly, numerous passive microwave devices, such as cavity resonators, waveguides, antennas, and filters, can be quickly prototyped and manufactured using additive manufacturing. In a way, 3D printing has opened the door for exploring an unlimited number of design geometries, and we are only limited now by devising new passive microwave circuits to make use of 3D printing.



(a)



(b)

Fig. 6. Red Horn Antenna Measured (a) Radiation Pattern and (b) Return Loss.

REFERENCES

- [1] M. I. M. Ghazali, K. Y. Park, V. Gjokaj, A. Kaur, and P. Chahal, "3d printed metallized plastic waveguides for microwave components," *International Symposium on Microelectronics*, vol. 2017, no. 1, pp. 000 078–000 082, Oct. 2017.
- [2] J. Shen, M. Aiken, C. Ladd, M. D. Dickey, and D. S. Ricketts, "A simple electroless plating solution for 3d printed microwave components," in *2016 Asia-Pacific Microwave Conference (APMC)*. IEEE, Dec. 2016, pp. 1–4.
- [3] C. A. Balanis, *Antenna theory analysis and design*. Hoboken, New Jersey Wiley, 2016.